

Original Article

Conjugation of arginylglycylaspartic acid to human serum albumin decreases the tumor-targeting effect of albumin by hindering its secreted protein acidic and rich in cysteine-mediated accumulation in tumors

Cho Rong Park^{1,2,5}, Myung Geun Song^{1,6}, Ji-Yong Park^{1,5}, Hyewon Youn^{1,2,7,8}, June-Key Chung^{1,2,3,5,8,9}, Jae Min Jeong^{1,2,3,5}, Yun-Sang Lee^{1,3}, Gi Jeong Cheon^{1,2,3,4}, Keon Wook Kang^{1,2,3,4,5}

¹Department of Nuclear Medicine, ²Cancer Research Institute, ³Institute of Radiation Medicine, Medical Research Center, ⁴Tumor Biology Program, Seoul National University College of Medicine, Seoul, Korea; ⁵Department of Biomedical Sciences, Seoul National University Graduate School, Seoul, Korea; ⁶Biomedical Research Institute, ⁷Cancer Imaging Center, Seoul National University Hospital, Seoul, Korea; ⁸Tumor Microenvironment Global Core Research Center, Seoul National University, Seoul, Korea; ⁹National Cancer Center, Goyang, Korea

Received October 6, 2019; Accepted April 7, 2020; Epub June 15, 2020; Published June 30, 2020

Abstract: Human serum albumin (HSA) accumulates in tumors by the enhanced permeability and retention (EPR) effect, which is a passive targeting effect in tumors. A recent study showed that secreted protein acidic and rich in cysteine (SPARC), an albumin-binding protein, mediates albumin accumulation in tumors. Arg-Gly-Asp (RGD) is a peptide targeting integrin $\alpha_v\beta_3$, which is highly expressed during tumor angiogenesis. We investigated whether conjugation of RGD to HSA could synergistically enhance tumor targeting. Accumulation of cRGDyK-HSA in integrin $\alpha_v\beta_3$ -expressing SK-OV3 cells was observed by confocal microscopy. In SK-OV3 cells overexpressing the albumin binding protein SPARC, cellular uptake of HSA increased, but uptake of cRGDyK-HSA did not. cRGDyK-HSA showed decreased tumor accumulation compared with HSA by positron emission tomography (PET) scanning and biodistribution studies in an SK-OV3 xenograft mouse model. In SK-OV3 tumors, HSA accumulation colocalized with SPARC expression, while cRGDyK-HSA only accumulated in the outer region of the tumor, even though SPARC and integrin $\alpha_v\beta_3$ were expressed within the tumor core. We speculate that cRGDyK conjugation to HSA changes the characteristics of HSA and hinders its tumor-targeting effect. Therefore, HSA should be modified to preserve its native characteristics and enhance the tumor-targeting effects of HSA conjugates.

Keywords: Human serum albumin, RGD, SPARC, EPR effect, tumor targeting

Introduction

Human serum albumin (HSA) is the most abundant protein in humans (60% of blood plasma protein); this is the main advantage of using albumin as a nanocarrier [1]. HSA can accumulate in tumors by the enhanced permeability and retention (EPR) effect [2, 3]. HSA accumulation in tumors primarily occurs by simple infiltration, not by receptor-mediated uptake [4-6]. While albumin is generally thought to infiltrate into tumors by the EPR effect, some studies propose that albumin binding proteins and receptors mediate albumin uptake into tumors [7]. Some studies suggest that secreted pro-

tein acidic and rich in cysteine (SPARC) can sequester albumin in the tumor stroma and contribute to the tumor-specific uptake of albumin [8, 9]. SPARC is an albumin binding protein and is highly expressed in some cancers [10, 11]. A recent study showed that SPARC can enhance HSA accumulation in SPARC-expressing gliomas by an active targeting mechanism [12].

Tumor angiogenesis is a hallmark of cancer, and integrin $\alpha_v\beta_3$ is a highly specific angiogenic marker [13]. Arg-Gly-Asp (RGD) is an integrin $\alpha_v\beta_3$ -targeting peptide that was identified from fibronectin [14, 15]. Active tumor targeting

Conjugation of RGD to albumin hinders its SPARC-mediated accumulation in tumors

strategies using RGD or modified RGD peptides have already been implemented in preclinical and clinical studies by other investigators [16-18].

In this study, we investigated whether conjugation of RGD to HSA could enhance the tumor-targeting ability of native HSA via a combination effect.

Materials and methods

Conjugation of DBCO and cRGDyK to HSA

HSA was fluorescently labeled with FNR648 as described in our previous publication [19]. The purified dibenzocyclooctyne (DBCO)-HSA was reacted with azido cyclic RGDyK (N_3 -cRGDyK, 1.4 mg/mL, dissolved in PBS) in 1 mL of PBS at a molar ratio of 1:6 for 30 min at 37°C. HSA-cRGDyK conjugates were further purified using PD-10 columns (GE Healthcare, Buckinghamshire, UK) and eluted with PBS. At each step, the protein concentration was measured with a bicinchoninic acid (BCA) protein assay kit (Pierce Endogen, Rockford, IL, USA), and the samples were analyzed by matrix-assisted laser desorption/ionization-time of flight (MALDI-TOF) using the TOF-TOF 5800 System (AB SCIEX, Framingham, MA, USA) at every conjugation step.

Radiolabeling of DBCO-HSA and cRGDyK-HSA

DBCO-HSA and cRGDyK-HSA were radiolabeled using a previously published method [19].

Cell culture

The human cancer cell lines SK-OV3 (ovarian cancer), PC3 (prostate cancer), DU145 (prostate cancer), 22Rv1 (prostate cancer), and KB (head and neck cancer) were grown in RPMI medium (Welgene, Daegu, South Korea) containing 10% (v/v) fetal bovine serum (FBS; Thermo Fisher Scientific, Grand Island, NY, USA) and 1% antibiotics (Thermo Fisher Scientific). Cells were incubated in a 37°C humidified incubator with a 5% CO₂ atmosphere.

Generation of SPARC-overexpressing cell lines

SPARC-bio-His was a gift from Gavin Wright (Addgene plasmid #52078; <http://n2t.net/addgene:52078>); RRID: Addgene_52078) [20].

Cells were seeded in 100 mm dishes with antibiotic-free medium and transfected with Lipofectamine 2000 (Thermo Fisher Scientific) according to the manufacturer's instructions. Cells were harvested 48 h after transfection and seeded for confocal microscopy imaging of HSA and cRGDyK-HSA uptake in cells.

Reverse transcriptase-polymerase chain reaction (RT-PCR)

Total RNA was purified from cells with TRIzol reagent (Thermo Fisher Scientific). For cDNA synthesis, amfiRivert Platinum cDNA synthesis Master Mix (GenDEPOT, Barker, TX, USA) was used with 2 µg of mRNA following the manufacturer's instructions. From synthesized cDNA, the mRNA levels of integrin α_v , β_3 , SPARC, and β -actin were measured. The sequences of the forward and reverse primers for integrin α_v were 5'-GAA AAG AAT GAC ACG GTT GC-3' and 5'-TAA CCA ATG TGG AGT TGG TG-3', which yields a product size of 318 base pairs. The sequences of the forward and reverse primers for integrin β_3 were 5'-CAG ACT TGG GCA GGG TAC AG-3' and 5'-GAC CTT CAA GAC TGG CTG CT-3', which yields a product size of 396 base pairs. The sequences of the forward and reverse primers of β -actin were 5'-ACC AGG GCT GCT TTT AAC TCT-3' and 5'-GAG TCC TTC CAC GAT ACC AAA-3'. The PCR was run as follows: an initial single hold step of 94°C for 5 min, followed by 30 cycles of 30 sec at 94°C and 1 min at the annealing temperature, and a final hold step at 72°C for 10 min. The annealing temperature for integrin α_v was 62°C, and the annealing temperature for integrin β_3 and β -actin was 58°C. PCR products were analyzed by gel electrophoresis in 1.2% agarose gels and visualized by staining with Loading Star (DyneBio Inc, Seoul, South Korea).

Western blotting

Total protein was isolated from cells using radioimmunoprecipitation assay buffer (Sigma-Aldrich, St. Louis, MO, USA) and a protease inhibitor cocktail (Roche, Nutley, NJ, Switzerland) and quantified using a BCA protein assay kit. Each sample (20 µg of lysate) was loaded onto an SDS-PAGE gel. After electrophoresis, the gels were blotted onto polyvinylidene di-

Conjugation of RGD to albumin hinders its SPARC-mediated accumulation in tumors

fluoride (PVDF) membranes (Millipore, Watford, UK). The PVDF membranes were blocked with 5% skim milk in Tris-buffered saline containing Tween-20 (TBST) for 1 h at room temperature. The membranes were incubated overnight at 4°C with primary antibodies against integrin α_v (sc-9969, Santa Cruz Biotechnologies, Santa Cruz, CA, USA; diluted 1:200), integrin β_3 (#13166, Cell Signaling Technology, Danvers, MA, USA; diluted 1:1000), SPARC (#5420, Cell Signaling Technology; diluted 1:1000), and β -actin (A5441, Sigma-Aldrich; diluted 1:5000). Membranes were then probed with horseradish peroxidase (HRP)-conjugated anti-rabbit or anti-mouse IgG (Cell Signaling Technologies). Visualization was performed using enhanced chemiluminescence (ECL) reagents (Roche). The signal intensity was measured using an LAS-3000 imaging system (Fujifilm, Tokyo, Japan).

Confocal microscopy imaging for cell binding analysis

For immunofluorescence analysis, 1.5×10^5 cells (SK-OV3 or SK-OV3-SPARC) were seeded in 12-well plates (Nalge NUNC International, Naperville, IL, USA) overnight. For staining, all procedures used 1% bovine serum albumin (BSA; g/v) in Hank's Balanced Salt Solution (HBSS, Thermo Fisher Scientific). Cells were incubated with 2 nmol of FNR648-labeled HSA or cRGDyK-HSA for 2 h. For blocking with cold cRGDyK, the cells were treated with a 500-fold higher concentration of deprotected cRGDyK (FutureChem, Seoul, South Korea) than that of cRGDyK-HSA. For blocking with cold HSA, the cells were coincubated with 1000 nmole HSA (a 500-fold higher concentration than that of FNR648-HSA). Cells were washed three times and then fixed using paraformaldehyde (Santa Cruz Biotechnologies). The slides were mounted with Prolong Gold reagent (Thermo Fisher Scientific). Fluorescence images were taken on a confocal laser scanning microscope (Leica TCS SP8, Wetzlar, Hesse, Germany). Five images were acquired from three independent experiments and used to quantify FNR648-HSA uptake by the cells. Images were selected with similar total numbers of cells. The average signal intensity of FNR648-HSA or FNR648-cRGDyK-HSA in each image was measured using the LAS X program, and the

numbers of 4',6-diamidino-2-phenylindole (DAPI)-positive cells in the images were counted. The average signal intensity of FNR648-HSA or FNR648-cRGDyK-HSA was divided by the number of DAPI-positive cells, which represents the number of viable cells in the image. This ratio was used to quantify FNR648-HSA or FNR648-cRGDyK-HSA uptake in cells.

Animal model and PET imaging

All animal studies were performed under approval from the Seoul National University Institutional Animal Care and Use Committee (IACUC No. 14-0028). BALB/c nude mice (5 weeks old, female) were purchased from Orient Bio Inc., (Seongnam, South Korea). SK-OV3 cells (2×10^6) were injected subcutaneously into the right lower flanks. Tumors were grown to a size of 5-10 mm in diameter.

Small animal PET imaging of tumor-bearing mice was performed using PETbox (SOFIE Bioscience, Culver, CA, USA). Mice were injected with 0.37-0.74 MBq of ^{64}Cu -HSA or ^{64}Cu -cRGDyK-HSA (1.5-3 nmole for ^{64}Cu -HSA; 3.5-3.8 nmole for ^{64}Cu -cRGDyK-HSA) via the tail vein. At 10 min and 4, 24, and 48 h after injection, the mice were anesthetized with 2% isoflurane and placed in the prone position. Static scans (10-minute scans at 10 min and 4 h after injection; 20-minute scans at 24 and 48 h after injection) were obtained, and the images were reconstructed using the AMIDE algorithm. Reconstructed data from PETbox were visualized and coregistered using InVivoScope (Bio-scan, Washington, DC, USA).

Biodistribution studies

For biodistribution studies, mice bearing SK-OV3 xenografts ($n = 6$ for each group) were injected with 0.37 MBq of ^{64}Cu -HSA or ^{64}Cu -cRGDyK-HSA via the tail vein and sacrificed at each time point (10 min, 4 h, and 24 h) postinjection. Tumors and normal tissues were excised and weighed, and their radioactivity was measured using a γ -counter. The radioactivity uptake in the tumor and normal tissues was expressed as the percent injected dose per gram (%ID/g).

Immunofluorescence analysis of tumor tissues

For immunofluorescence analysis of tumor tissues, the tumors were embedded in OCT com-

Conjugation of RGD to albumin hinders its SPARC-mediated accumulation in tumors

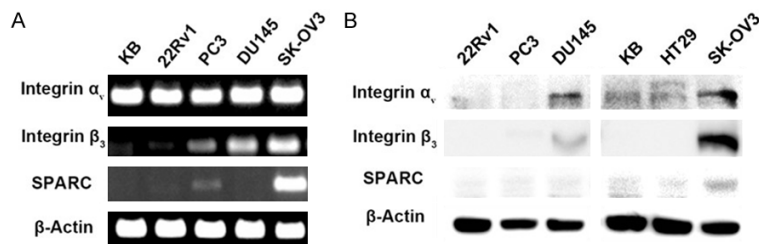


Figure 1. Integrin α_v , integrin β_3 , and SPARC expression in cells. To examine the expression of integrin α_v , integrin β_3 , and SPARC in tumor cell lines, several cell lines were examined. A, B. RT-PCR and Western blotting were used to observe the mRNA and protein expression levels of each target gene or protein.

pond and frozen, and 4- μ m thick serial coronal sections were mounted on slides. Tumor sections were fixed with acetone. Sections were incubated in 5% (g/v) BSA containing PBS for 1 h at room temperature. The slides were incubated overnight with the following antibodies: anti-human integrin $\alpha_v\beta_3$ (Bioss, Woburn, Massachusetts, USA; diluted 1:200) or anti-human SPARC (R & D Systems, Minneapolis, MN, USA; diluted 1:200). Tissue was then incubated with secondary antibody for 1 h at room temperature (Alexa Fluor 488-conjugated anti-goat or anti-rabbit antibody; diluted 1:400). After antibody staining, the slides were mounted with Prolong Gold reagent with DAPI (Thermo Fisher Scientific). Fluorescence was detected using a Leica TCS SP8 confocal laser scanning microscope.

Statistical analysis

Data were analyzed as the mean \pm standard deviation and using the Mann-Whitney U-test. A *P*-value of less than 0.05 was considered statistically significant. Statistical analyses were performed using GraphPad Prism version 5.0 (GraphPad).

Results

Integrin $\alpha_v\beta_3$ expression in cell lines

To confirm the targeting efficiency of cRGDyK-HSA, an integrin $\alpha_v\beta_3$ -expressing cell line was selected by RT-PCR and Western blot analysis. RT-PCR (Figure 1A) and Western blot (Figure 1B) analysis demonstrated that SK-OV3, the human ovarian cancer cell line, had the highest integrin $\alpha_v\beta_3$ expression among the five |

cell lines. We also evaluated SPARC expression since it affects the tumor accumulation of HSA. SK-OV3 cells expressed SPARC at a low level.

^{64}Cu labeling of cRGDyK-HSA

cRGDyK-HSA was radiolabeled using the click reaction, according to a previously published method. ^{64}Cu was well radiolabeled in 3-azidopropyl-NOTA (Figure 2B). ^{64}Cu -labeled 3-azidopropyl-NOTA was conjugated to HSA and cRGDyK-HSA. ^{64}Cu -HSA and ^{64}Cu -cRGDyK-HSA were successfully radiolabeled (Figure 2C and 2E), and free ^{64}Cu was not observed after the purification step (Figure 2D and 2F).

Cellular uptake of cRGDyK-HSA

To observe the SPARC- or integrin $\alpha_v\beta_3$ -dependent cellular uptake of cRGDyK-HSA, SK-OV3 cells were treated with fluorescently labeled HSA or cRGDyK-HSA. The cellular uptake of HSA or cRGDyK-HSA was observed as a fluorescence signal on confocal images. cRGDyK-HSA showed a higher uptake than HSA in SK-OV3 cells (Figure 3A and 3B). For objective comparison, fluorescent staining was quantified. HSA showed decreased cellular uptake when the cells were blocked with excess HSA (Figure 3C, *P* < 0.01). Blocking with cRGDyK resulted in decreased cellular uptake of cRGDyK-HSA (Figure 3D, *P* < 0.001). However, blocking with HSA had no effect on the cellular uptake of cRGDyK-HSA (Figure 3D). To verify the role of SPARC in cRGDyK-HSA uptake, HSA and cRGDyK-HSA uptake were evaluated in SPARC-overexpressing SK-OV3 cells (SK-OV3-SPARC) because SK-OV3 cells endogenously express low levels of SPARC (Figure 1A and 1B). SK-OV3-SPARC cells showed HSA-specific uptake of HSA (Figure 4C, *P* < 0.01) and cRGDyK-specific uptake of cRGDyK-HSA. cRGDyK-HSA uptake was not affected by blocking HSA (Figure 4D, *P* < 0.05). When the two probes (HSA and cRGDyK-HSA) were compared, HSA uptake was significantly increased in SK-OV3-SPARC cells compared with parental SK-OV3 cells (Figure 4E, *P* < 0.01). With respect to cRGDyK-HSA uptake, no difference was found

Conjugation of RGD to albumin hinders its SPARC-mediated accumulation in tumors

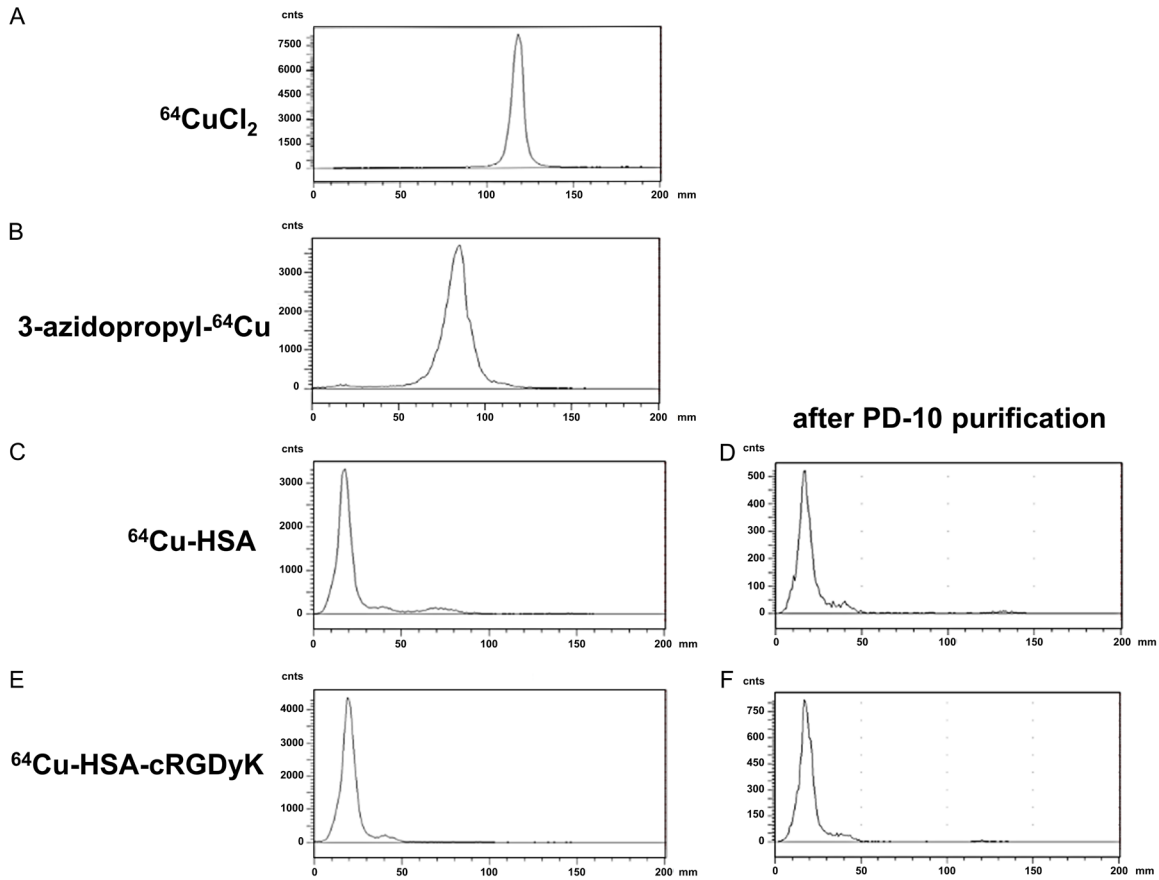
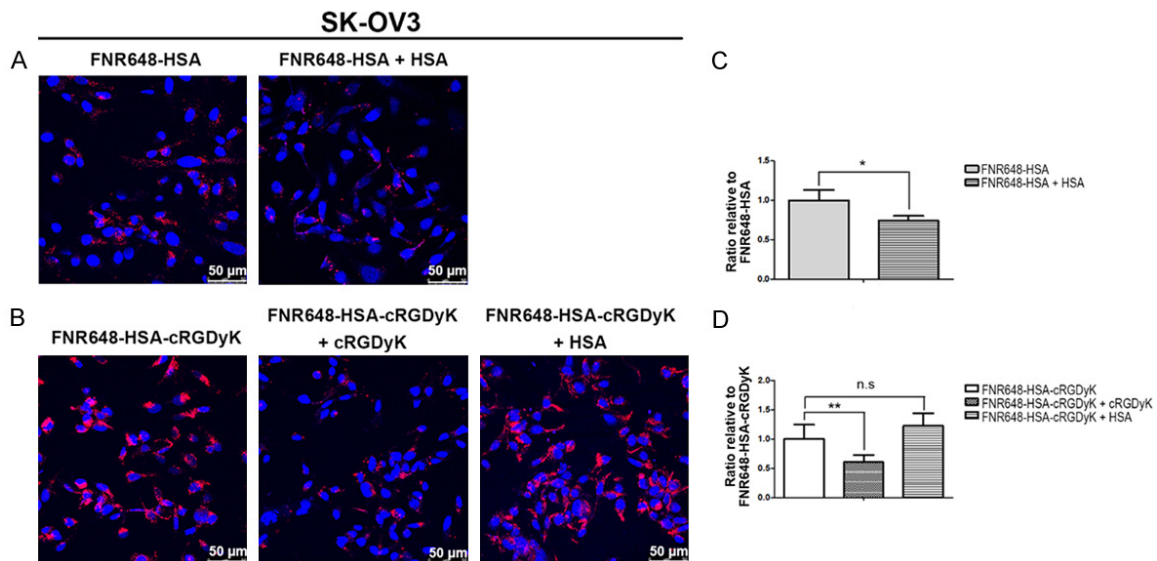


Figure 2. ^{64}Cu radiolabeling efficiency of HSA and HSA-cRGDyK. For radiolabeling of HSA and HSA-cRGDyK with ^{64}Cu , each radiolabeling step was confirmed using thin-layer chromatography in 0.1 M citric acid. A. Free ^{64}Cu chromatography data for comparing the radiolabeling efficiency. B. ^{64}Cu radiolabeling analysis of 3-azidopropyl showed that 3-azidopropyl was efficiently radiolabeled with ^{64}Cu (RF: 0.8). C. Radiolabeling of HSA using 3-azidopropyl- ^{64}Cu . D. ^{64}Cu -HSA after the purification step. E. Radiolabeling of HSA-cRGDyK using 3-azidopropyl- ^{64}Cu . F. ^{64}Cu -HSA-cRGDyK after the purification step. 3-Azidopropyl- ^{64}Cu (RF: 0.8) or free ^{64}Cu (RF: 1.1) was present in ^{64}Cu -HSA and ^{64}Cu -HSA-cRGDyK.



Conjugation of RGD to albumin hinders its SPARC-mediated accumulation in tumors

Figure 3. HSA-cRGDyK uptake in SK-OV3 cells is dependent on cRGDyK. Integrin $\alpha_v\beta_3$ -expressing SK-OV3 cells were treated with fluorescently labeled HSA or HSA-cRGDyK. A. Representative cell images of HSA uptake in cells. B. Representative images of HSA-cRGDyK uptake in cells. C. Quantification of HSA uptake in cells from confocal images. D. Quantification of HSA-cRGDyK uptake in cells from confocal images. The quantification method is well described in the materials and methods. Confocal microscopy imaging was used for cell binding analysis. Because of the decreased HSA-cRGDyK uptake in the cRGDyK-treated group (FNR648-HSA-cRGDyK + cRGDyK, $P < 0.01$), we speculated that HSA-cRGDyK showed cRGDyK-specific uptake in SK-OV3 cells (*: $P < 0.05$, **: $P < 0.01$).

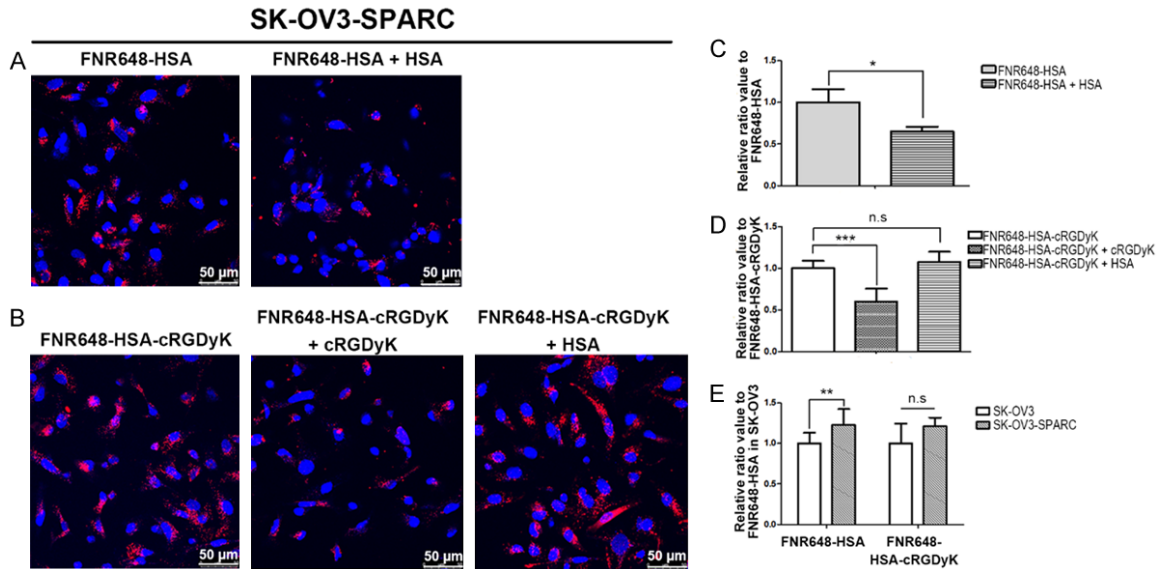


Figure 4. HSA and HSA-cRGDyK uptake in SPARC-overexpressing SK-OV3 cells compared to SK-OV3 cells. SPARC-overexpressing SK-OV3 cells (SK-OV3-SPARC) were treated with HSA and HSA-cRGDyK. A. Representative confocal images of HSA-treated SK-OV3 SPARC cells. B. Cellular confocal images of HSA-cRGDyK-treated SK-OV3-SPARC cells. C. Quantification of HSA uptake in cells from confocal images. D. Quantification of HSA-cRGDyK uptake in cells from confocal images. E. Quantification of FNR648-HSA and FNR648-HSA-cRGDyK uptake in SK-OV3 and SK-OV3-SPARC cells. The cellular uptake of each probe in parental SK-OV3 cells was set to 1.0. In the case of HSA, SK-OV3-SPARC cells showed higher uptake of HSA than SK-OV3 cells, but there was no difference in HSA-cRGDyK cellular uptake. *: $P < 0.05$, ***: $P < 0.001$.

between SK-OV3 and SK-OV3-SPARC cells (Figure 4E).

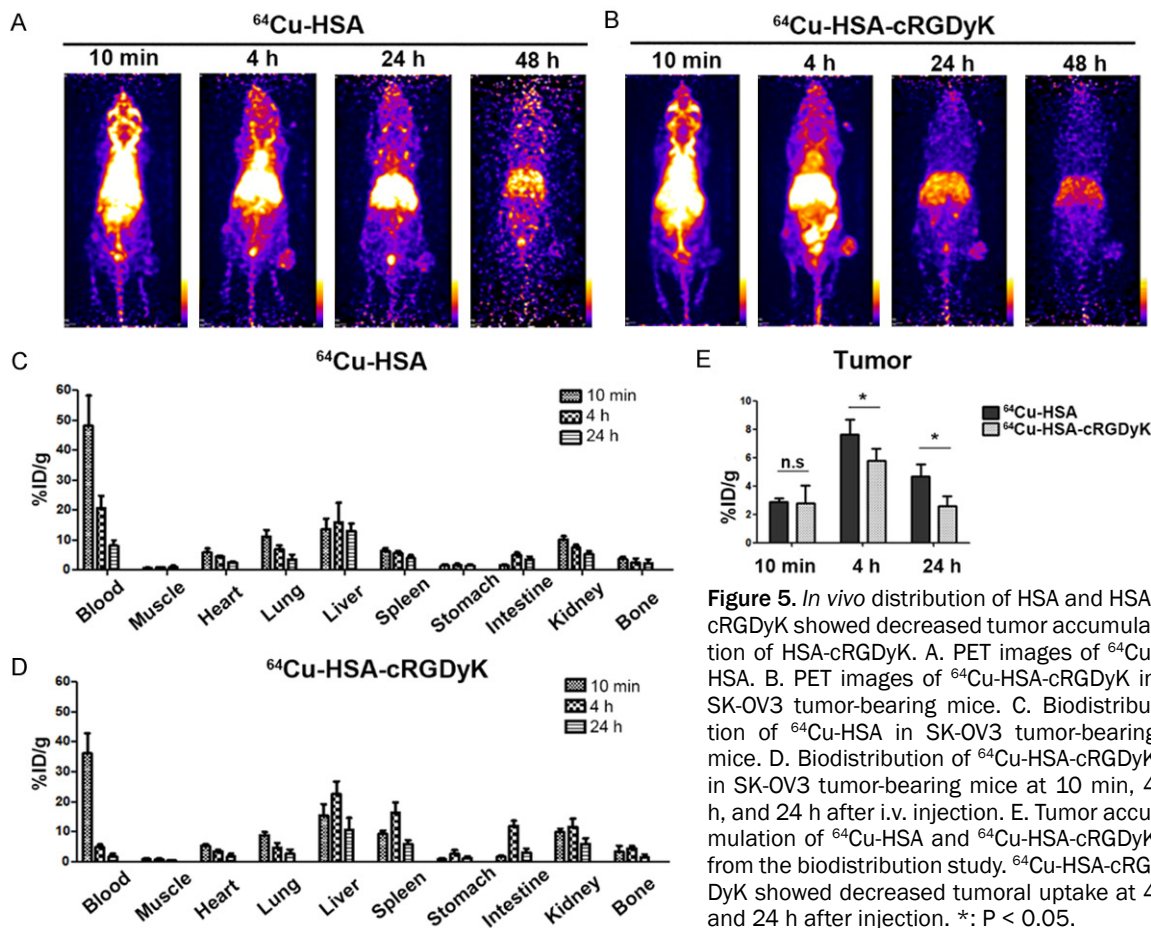
The distribution of ^{64}Cu -HSA and ^{64}Cu -cRGDyK-HSA *in vivo*

To evaluate the *in vivo* distribution and tumor targeting of cRGDyK-HSA, SK-OV3 tumor-bearing mice were injected with ^{64}Cu -cRGDyK-HSA, and PET images were acquired at 10 min and 4, 24, and 48 h after injection. PET images from mice injected with ^{64}Cu -HSA were also acquired for comparison with cRGDyK-HSA. The PET signal in the tumor (the right thigh of the mice) was similar for ^{64}Cu -HSA and ^{64}Cu -cRGDyK-HSA (Figure 5A and 5B). A biodistribution study was performed to observe the organ distribution and tumor accumulation of ^{64}Cu -HSA and ^{64}Cu -cRGDyK-HSA (Figure 5C-E). In the blood,

^{64}Cu -cRGDyK-HSA showed less accumulation than ^{64}Cu -HSA at 4 and 24 h after injection (Figure 5C and 5D, $P < 0.01$). More ^{64}Cu -cRGDyK-HSA than ^{64}Cu -HSA accumulated in the reticuloendothelial organs (RES organs; the spleen and liver) (Figure 5C and 5D), especially at 4 h after injection ($P < 0.05$ for liver and $P < 0.01$ for spleen at 4 h). This biodistribution pattern was consistent with the PET images, which showed longer persistence of ^{64}Cu -HSA than ^{64}Cu -cRGDyK-HSA in the circulation. The tumor accumulation of ^{64}Cu -cRGDyK-HSA was lower than that of ^{64}Cu -HSA (Figure 5E, $P < 0.05$ for 4 and 24 h).

Colocalization of HSA and cRGDyK-HSA in the tumor tissue

To determine the cause of the reduced accumulation of cRGDyK-HSA in tumors, the colo-



calization of HSA and cRGDyK-HSA in tumors was observed. SK-OV3 tumor-bearing mice were injected with HSA or cRGDyK-HSA, and tumor tissues were collected at 4 h after injection, which was the time point at which the accumulation in tumors was the highest. The distribution of cRGDyK-HSA was compared with the expression of integrin $\alpha_v\beta_3$ or SPARC in the tumors (Figure 6). In the outer region of the tumor, cRGDyK-HSA accumulation was observed, and this distribution was associated with the expression of integrin $\alpha_v\beta_3$ (Figure 6B). However, in the core of the tumor, although integrin $\alpha_v\beta_3$ expression was observed, cRGDyK-HSA accumulation was significantly reduced (Figure 6C). The tumor distribution of cRGDyK-HSA was also compared with SPARC expression. Even though SPARC was expressed in the tumor core, cRGDyK-HSA did not accumulate there (Figure 6F). The distribution of HSA in SK-OV3 tumors was then compared with SPARC expression (Figure 7). In HSA-injected mice, HSA accumulation in the tumor corre-

lated with SPARC expression (Figure 7B and 7C).

Discussion

Many studies on tumor targeting using HSA have revealed that the EPR effect primarily mediates HSA accumulation in tumors. However, some studies have shown other mechanisms of HSA accumulation in tumors, including albumin binding receptors or protein-mediated transport. One albumin binding protein, SPARC, contributes to HSA accumulation in tumors. Our recent study showed that SPARC enhances HSA accumulation in SPARC-expressing gliomas [12]. In this study, we evaluated the tumor-targeting ability of HSA-conjugated RGD, a moiety targeting integrin $\alpha_v\beta_3$.

We observed the cellular uptake of cRGDyK-HSA *in vitro* and demonstrated that cRGDyK-HSA was taken up into cells in a cRGDyK-dependent manner, independent of SPARC ex-

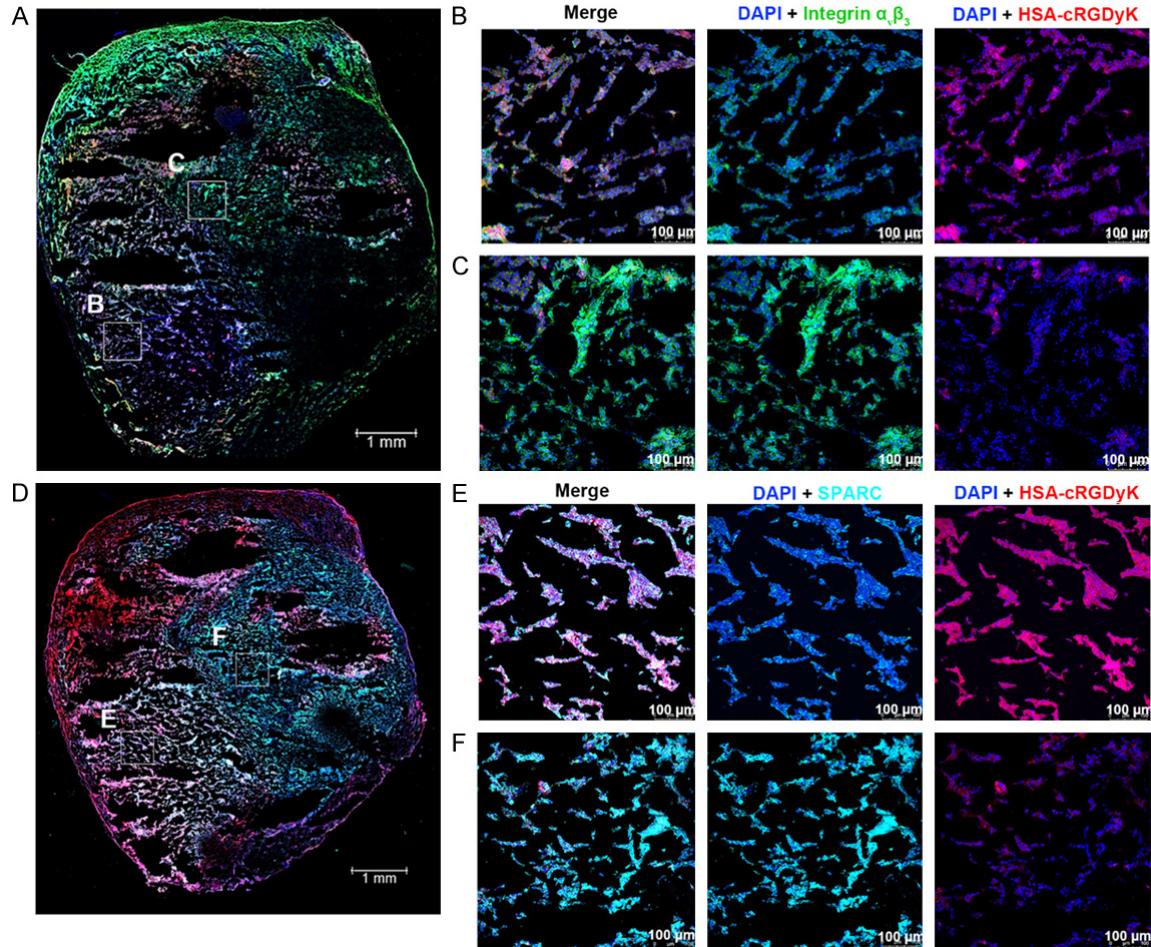


Figure 6. Colocalization analysis of HSA-cRGDyK was RGD-dependent but hindered SPARC-dependent accumulation in tumors. To determine the effect of HSA-cRGDyK distribution, SK-OV3 tumor tissues were stained with an anti-integrin $\alpha_v\beta_3$ antibody or a SPARC antibody. A-C. Integrin $\alpha_v\beta_3$ staining in tumor images. A. Whole tumor immunofluorescence images. B. Colocalization of HSA-cRGDyK and integrin $\alpha_v\beta_3$ in the outer region of the tumor. C. Colocalization of HSA-cRGDyK and integrin $\alpha_v\beta_3$ in the inner region of the tumor. HSA-cRGDyK showed integrin $\alpha_v\beta_3$ -dependent tumor accumulation. D-F. SPARC antibody-stained tumor images. D. Total tumor immunofluorescence images. E. Colocalization of HSA-cRGDyK and SPARC in the outer region of the tumor. F. Colocalization of HSA-cRGDyK and SPARC in the inner region of the tumor. Tumor region F, which highly expresses SPARC, showed decreased HSA-cRGDyK accumulation. Red, HSA-cRGDyK; green, integrin $\alpha_v\beta_3$; light blue, SPARC; dark blue, cell nuclei stained with DAPI. Each image is labeled with its scale bar, 1 mm or 100 μm .

pression (Figures 3 and 4). *In vivo* PET images and biodistribution data showed that the tumor-targeting effect of ^{64}Cu -cRGDyK-HSA was decreased compared with that of ^{64}Cu -HSA (Figure 5). Colocalization studies of HSA and cRGDyK-HSA showed that even though integrin $\alpha_v\beta_3$ was expressed within the tumor core, cRGDyK-HSA accumulated in the outer region of the tumor. SPARC was also expressed in the tumors, but the expression of SPARC did not affect the accumulation of cRGDyK-HSA in the tumor core (Figure 6). By contrast, HSA distribution correlated with SPARC expres-

sion (Figure 7). From these results, we conclude that the accumulation of cRGDyK-HSA was mediated by integrin $\alpha_v\beta_3$; however, SPARC-mediated HSA accumulation in tumors was decreased by conjugation of cRGDyK to HSA.

The loss of the native characteristics of HSA in cRGDyK-HSA was also shown by the PET images and the biodistribution study. ^{64}Cu -cRGDyK-HSA accumulated less in the blood than ^{64}Cu -HSA and showed faster clearance through the liver and intestine (Figure 5). These data

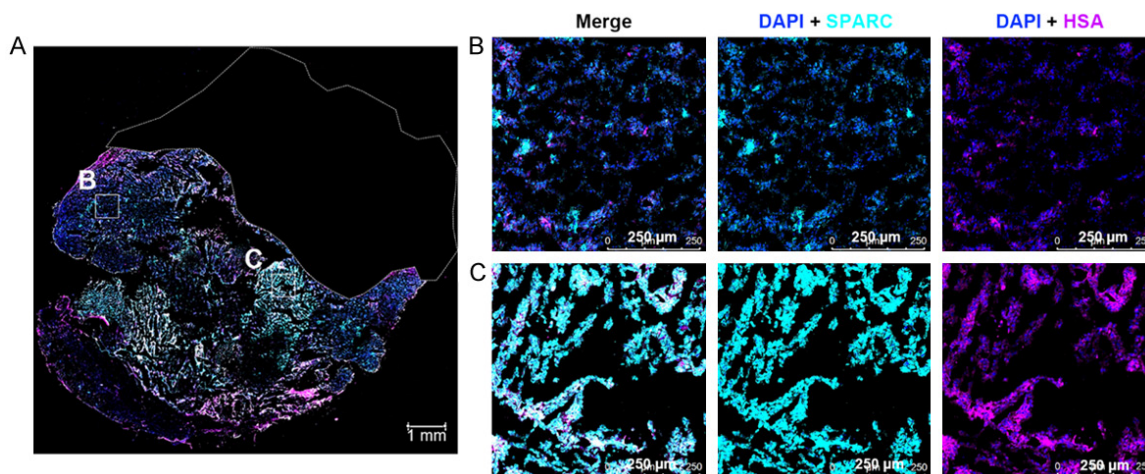


Figure 7. Colocalization analysis of HSA showed SPARC-dependent tumor accumulation of HSA. To determine the effect of SPARC expression, tumor tissue was stained with an anti-SPARC antibody. A. Immunofluorescence image of a whole tumor from a Cy3-HSA-injected mouse. B, C. Magnified images of two different tumor regions. Region C of the tumor, which highly expresses SPARC, showed high accumulation of HSA. Magenta, Cy3-HSA; light blue, SPARC; dark blue, DAPI. Each image is labeled with its scale bar, 1 mm or 250 μm .

Table 1. MALDI-TOF analysis for characterization of HSA and HSA-cRGDyK

| | Molecular Weight | (-) HSA Molecular Weight | Molar Ratio (DBCO/HSA) |
|------------|-----------------------|-------------------------------|--------------------------|
| DBCO-HSA | 69848.14 \pm 194.25 | 3184.14 \pm 194.25 | 6.72 \pm 0.41 |
| | Molecular Weight | (-) DBCO-HSA Molecular Weight | Molar Ratio (cRGDyK/HSA) |
| HSA-cRGDyK | 74210.17 \pm 824.49 | 4726.03 \pm 675.11 | 5.29 \pm 0.76 |

suggest that cRGDyK-HSA is not recognized as native HSA and is eliminated from the body. To conjugate cRGDyK to HSA, we used a fine-tuned click chemistry-based albumin nanoplat-form (CAN), which was published by our group [19]. We showed that CAN conserves the bio-compatibility and long half-life of HSA in the circulation *in vivo* [1]. The difference between native HSA and cRGDyK-HSA was that cRGDyK-HSA contains 5.29 RGDs per molecule of HSA (Table 1). Our previous study proved that SPARC mediates the active targeting of HSA, especially in the inner region of the tumor, which cannot be reached by the EPR effect [12]. In this study, even though the tumors expressed SPARC, cRGDyK-HSA did not reach the tumor core. It can be speculated that the characteristics of native HSA that allow SPARC-mediated active targeting to the tumor core to occur are lost in cRGDyK-HSA, such that it only accumulates in the outer region of the tumor. After cRGDyK-HSA accumulates in the outer region of the tumor via the EPR effect, integrin $\alpha_v\beta_3$ mediates its cellular internalization. We expected

that cRGDyK-HSA would enhance its accumulation in tumors by combining the EPR effect with active targeting via SPARC and integrin $\alpha_v\beta_3$. However, only the EPR effect and integrin $\alpha_v\beta_3$ -mediated accumulation of cRGDyK-HSA in tumors occurred, while SPARC-mediated accumulation was lost. From this result, it seems that HSA should be modified to preserve its native characteristics in tumor-targeting conjugates.

In summary, we developed cRGDyK-conjugated HSA as a tumor-targeting agent. cRGDyK-HSA showed enhanced tumor targeting ability mediated by integrin $\alpha_v\beta_3$ but not by SPARC *in vitro*. *In vivo* accumulation of cRGDyK-HSA in tumors was not enhanced compared with that of HSA. Based on our investigation of the localization of cRGDyK-HSA in tumor tissues, cRGDyK-HSA seems to lose the characteristics of native HSA as a result of cRGDyK conjugation. This results in decreased circulating HSA in the blood and decreased SPARC-mediated HSA accumulation in the tumor. From

these results, we conclude that HSA should be modified to conserve the characteristics of HSA and enhance the tumor-targeting effect of HSA conjugates.

Acknowledgements

We would like to thank the Korea Institute of Radiological & Medical Sciences for providing radioisotopes. Keon Wook Kang was supported by the Radiation Technology R & D program of the National Research Foundation of Korea funded by the Ministry of Science and Information and Communications Technology (ICT) (NRF-2017M2A2A7A01070923), and by the Framework of International Cooperation Program of the National Research Foundation of Korea (NRF-2017K2A9A2A10013554). Gi Jeong Cheon was supported by the National Research Foundation of Korea (NRF) grant funded by the Korea government (MSIT) (NRF-2017R1D1A1B03035648). Hyewon Youn was supported by the National Research Foundation of Korea (NRF) grant funded by the Korean government (MSIP) (NRF-2011-0030001 and NRF-2017R1A2B4012813).

Disclosure of conflict of interest

None.

Address correspondence to: Dr. Keon Wook Kang, Department of Nuclear Medicine, Seoul National University College of Medicine, 101, Daehak-Ro, Jongno-Gu, Seoul 03080, Korea. Tel: 82-2-2072-2803; Fax: 82-2-745-7690; E-mail: kangkw@snu.ac.kr; Dr. Myung Geun Song, Biomedical Research Institute, Seoul National University Hospital, Center for Medical Innovation, 71 Daehak-Ro, Jongno-Gu, Seoul 03082, Korea. Tel: 82-2-2072-4355; Fax: 82-2-2072-4352; E-mail: mgsong0310@gmail.com

References

- [1] Kratz F. Albumin as a drug carrier: design of prodrugs, drug conjugates and nanoparticles. *J Control Release* 2008; 132: 171-183.
- [2] Greish K. Enhanced permeability and retention (EPR) effect for anticancer nanomedicine drug targeting. *Methods Mol Biol* 2010; 624: 25-37.
- [3] Sinn H, Schrenk HH, Friedrich EA, Schilling U and Maier-Borst W. Design of compounds having an enhanced tumour uptake, using serum albumin as a carrier. Part I. *Int J Rad Appl Instrum B* 1990; 17: 819-827.
- [4] Langer K, Balthasar S, Vogel V, Dinauer N, von Briesen H and Schubert D. Optimization of the preparation process for human serum albumin (HSA) nanoparticles. *Int J Pharm* 2003; 257: 169-180.
- [5] Torchilin V. Tumor delivery of macromolecular drugs based on the EPR effect. *Adv Drug Deliv Rev* 2011; 63: 131-135.
- [6] Prabhakar U, Maeda H, Jain RK, Sevick-Muraca EM, Zamboni W, Farokhzad OC, Barry ST, Gabizon A, Grodzinski P and Blakey DC. Challenges and key considerations of the enhanced permeability and retention effect for nanomedicine drug delivery in oncology. *Cancer Res* 2013; 73: 2412-2417.
- [7] Merlot AM, Kalinowski DS and Richardson DR. Unraveling the mysteries of serum albumin: more than just a serum protein. *Front Physiol* 2014; 5: 299.
- [8] Fritzsche T, Schnolzer M, Fiedler S, Weigand M, Wiessler M and Frei E. Isolation and identification of heterogeneous nuclear ribonucleoproteins (hnRNP) from purified plasma membranes of human tumour cell lines as albumin-binding proteins. *Biochem Pharmacol* 2004; 67: 655-665.
- [9] Desai N, Trieu V, Damascelli B and Soon-Shiong P. SPARC expression correlates with tumor response to albumin-bound paclitaxel in head and neck cancer patients. *Transl Oncol* 2009; 2: 59-64.
- [10] Chlenski A and Cohn SL. Secreted Protein acidic and rich in cysteine. In: Schwab M, editors. *Encyclopedia of cancer*. Berlin, Heidelberg: Springer Berlin Heidelberg; 2017. pp. 4147-4151.
- [11] Nagaraju GP, Dontula R, El-Rayes BF and Lakka SS. Molecular mechanisms underlying the divergent roles of SPARC in human carcinogenesis. *Carcinogenesis* 2014; 35: 967-973.
- [12] Park CR, Jo JH, Song MG, Park JY, Kim YH, Youn H, Paek SH, Chung JK, Jeong JM, Lee YS and Kang KW. Secreted protein acidic and rich in cysteine mediates active targeting of human serum albumin in U87MG xenograft mouse models. *Theranostics* 2019; 9: 7447-7457.
- [13] Hanahan D and Weinberg RA. Hallmarks of cancer: the next generation. *Cell* 2011; 144: 646-674.
- [14] Pierschbacher MD and Ruoslahti E. Variants of the cell recognition site of fibronectin that retain attachment-promoting activity. *Proc Natl Acad Sci U S A* 1984; 81: 5985-5988.
- [15] Pierschbacher MD and Ruoslahti E. Cell attachment activity of fibronectin can be duplicated by small synthetic fragments of the molecule. *Nature* 1984; 309: 30-33.
- [16] Chen H, Niu G, Wu H and Chen X. Clinical application of radiolabeled RGD peptides for PET

Conjugation of RGD to albumin hinders its SPARC-mediated accumulation in tumors

- imaging of integrin $\alpha v \beta 3$. *Theranostics* 2016; 6: 78-92.
- [17] Hou J, Diao Y, Li W, Yang Z, Zhang L, Chen Z and Wu Y. RGD peptide conjugation results in enhanced antitumor activity of PD0325901 against glioblastoma by both tumor-targeting delivery and combination therapy. *Int J Pharm* 2016; 505: 329-340.
- [18] Yang G, Nie P, Kong Y, Sun H, Hou G and Han J. MicroPET imaging of tumor angiogenesis and monitoring on antiangiogenic therapy with an (^{18}F) labeled RGD-based probe in SKOV-3 xenograft-bearing mice. *Tumour Biol* 2015; 36: 3285-3291.
- [19] Park JY, Song MG, Kim WH, Kim KW, Lodhi NA, Choi JY, Kim YJ, Kim JY, Chung H, Oh C, Lee YS, Kang KW, Im HJ, Seok SH, Lee DS, Kim EE and Jeong JM. Versatile and finely tuned albumin nanoplatfom based on click chemistry. *Theranostics* 2019; 9: 3398-3409.
- [20] Sun Y, Vandenbrielle C, Kauskot A, Verhamme P, Hoylaerts MF and Wright GJ. A Human Platelet receptor protein microarray identifies the high affinity immunoglobulin e receptor subunit alpha (Fc ϵ 1) as an activating platelet endothelium aggregation receptor 1 (PEAR1) ligand. *Mol Cell Proteomics* 2015; 14: 1265-1274.